THE JOURNAL OF BIOLOGICAL CHEMISTRY
Vol. 278, No. 35, Issue of August 29, pp. 32753–32762, 2003
Printed in U.S.A.

Polyadenylation Regulates the Stability of *Trypanosoma brucei* Mitochondrial RNAs*

Received for publication, April 5, 2003, and in revised form, May 19, 2003
Published, JBC Papers in Press, June 11, 2003, DOI 10.1074/jbc.M303552200

Christopher M. Ryan‡, Kevin T. Militello‡§, and Laurie K. Read¶

From the Department of Microbiology and the Witebsky Center for Microbial Pathogenesis and Immunology, School of Medicine and Biomedical Sciences, State University of New York, Buffalo, New York 14214

Polyadenylation of RNAs plays a critical role in modulating rates of RNA turnover and ultimately in controlling gene expression in all systems examined to date. In mitochondria, the precise mechanisms by which RNAs are degraded, including the role of polyadenylation, are not well understood. Our previous *in organello* pulse-chase experiments suggest that poly(A) tails stimulate degradation of mRNAs in the mitochondria of the protozoan parasite *Trypanosoma brucei* (Militello, K. T., and Read, L. K. (2000) *Mol. Cell. Biol.* 21, 731–742). In this report, we developed an *in vitro* assay to directly examine the effects of specific 3′-sequences on RNA degradation. We found that a salt-extracted mitochondrial membrane fraction preferentially degraded polyadenylated mitochondrially and non-mitochondrially encoded RNAs over their non-adenylated counterparts. A poly(A) tail as short as 5 nucleotides was sufficient to stimulate rapid degradation, although an *in vivo* tail length of 20 adenosines supported the most rapid decay. A poly(U) extension did not promote rapid RNA degradation, and RNA turnover was slowed by the addition of uridine residues to the poly(A) tail. To stimulate degradation, the poly(A) element must be located at the 3′ terminus of the RNA. Finally, we demonstrate that degradation of polyadenylated RNAs occurs in the 3′ to 5′ direction through the action of a hydrolytic exonuclease. These experiments demonstrate that the poly(A) tail can act as a *cis*-acting element to facilitate degradation of *T. brucei* mitochondrial mRNAs.

The control of RNA stability is essential for the regulation of gene expression in all organisms (1–3). Polyadenylation at the 3′-ends of RNAs plays an important role in modulating rates of RNA turnover. However, the effect of 3′-poly(A) tails on RNA half-lives differs dramatically depending on the organism and subcellular compartment in which it occurs. In eukaryotic cytoplasm, poly(A) tails at the 3′-ends of mature mRNAs act in conjunction with the poly(A)-binding protein to stabilize mRNA (4). Conversely, polyadenylation destabilizes mRNA in bacteria (2, 5) and chloroplasts (3, 6). In these systems, poly(A) tails are added both to mature 3′ termini and to endonucleolytic cleavage products, subsequently signaling rapid decay of the corresponding RNAs.

The role of polyadenylation in the turnover of mitochondrial RNAs is not well understood. In plant mitochondria, polyadenylation has been reported to destabilize RNAs (7–9). Polyadenylated endonucleolytic cleavage products have not been detected in plant mitochondria, but polyadenylation of mature mRNA 3′-ends is correlated with reduced RNA abundance *in vivo* and promotes rapid RNA degradation *in vitro* (7, 9). Experiments performed in our laboratory using intact mitochondria from *Trypanosoma brucei* demonstrated that polyadenylation can also act to destabilize mRNAs in the mitochondria of this organism (10). The precise mechanisms by which polyadenylation acts to destabilize RNA remain undefined in both plant and trypanosome mitochondria. Interestingly, trypanosomes differ from bacteria, chloroplasts, and plant mitochondria in that a significant fraction of the steady-state mitochondrial mRNA population in trypanosomes is polyadenylated (2, 3, 5, 6, 11–16). Thus, although there are apparent similarities between trypanosomes and other organisms in which mRNA polyadenylation triggers rapid decay, poly(A)-mediated control of mitochondrial RNA stability in trypanosomes is likely to involve novel features.

Gene expression in *T. brucei* mitochondria involves a complex set of processes. Expression begins with the generation of polycistronic transcripts containing both mRNA and rRNA sequences (14, 17). Despite transcription of RNAs containing multiple open reading frames, mature monocistronic mRNAs vary in abundance depending on the life cycle stage of the parasite (12–16, 18–21). Thus, differential expression of specific mRNAs must be accomplished through post-transcriptional events. For example, polycistronic transcripts must be cleaved precisely at their 5′- and 3′-ends to release individual monocistronic mRNAs (14, 17). In addition, 12 of the 18 mRNAs encoded in *T. brucei* mitochondria undergo an extensive RNA editing process that creates start codons, stop codons, and open reading frames for otherwise untranslatable RNAs (22). As stated above, mRNAs are also polyadenylated at their 3′-ends. Polyadenylation in trypanosome mitochondria is a complex and poorly understood process in which the length of poly(A) tract is partially dependent on the edited status of the RNA (14–16). Northern blot analyses have revealed that RNAs detectable with unedited probes either lack a poly(A) tail (10) or contain short (~20 nucleotides) poly(A) tails (11, 12, 14–16, 21). RNAs detectable with probes corresponding to edited RNA sequences, as well as never edited mRNAs, may contain either short or long (~120–200 nucleotides) poly(A) tails (11, 12, 14–16, 21). The mechanisms by which RNA editing and polyadenylation are coordinated in trypanosome mitochondria are not known. However, we previously demonstrated that long poly(A) tails can be found on RNAs edited at as few as nine

* This work was supported in part by National Institutes of Health Grant AI47329 (to L. K. R.). The costs of publication of this article were defrayed in part by the payment of page charges. This article must therefore be hereby marked "*advertisement*" in accordance with 18 U.S.C. Section 1734 solely to indicate this fact.

‡ Supported in part by National Institutes of Health Training Grant AI07614.

§ Present address: Dept. of Immunology and Infectious Disease, Harvard School of Public Health, Boston, MA 02115.

¶ To whom correspondence should be addressed: Dept. of Microbiology, School of Medicine and Biomedical Sciences, SUNY, 138 Farber Hall, 3435 Main St., Buffalo, NY 14214. Tel.: 716-829-3307; Fax: 716-829-2158; E-mail: lread@acsu.buffalo.edu.

TABLE I
Primers used for PCR to generate templates for in vitro transcription
Sequences in boldface indicate T7 promoter sequence. S, sense; AS, antisense.

RNA	Polarity	Primer Sequence
All pBSC	S	5′-**GTAATACGACTCACTATAGGGC**-3′
pBSC-A20	AS	5′-TTTTTTTTTTTTTTTTTTTTGATCCCCCGGGCTGC-3′
All RPS12un	S	5′-**TGTAATACGACTCACTATAGGG**CTAATACACTTTTGATAACAAACTAAAGTAAA-3′
RPS12un	AS	5′-AAAAACATATCTTATTCT-3′
RPS12un-A5	AS	5′-TTTTTAAAAACATATCTTATTCT-3′
RPS12un-A10	AS	5′-TTTTTTTTTTAAAAACATATCTTATTCT-3′
RPS12un-A15	AS	5′-TTTTTTTTTTTTTTTAAAAACATATCTTATTCT-3′
RPS12un-A20	AS	5′-TTTTTTTTTTTTTTTTTTTTAAAAACATATCTTATTCT-3′
RPS12un-A30	AS	5′-TTTTTTTTTTTTTTTTTTTTTTTTTTTTTTAAAAACATATCTTATTCT-3′
RPS12un-U20	AS	5′-AAAAAAAAAAAAAAAAAAAAAAAAAACATATCTTAT-3′
RPS12un-AU	AS	5′-TTTTTTTAAAATTTTTTTTTAAAAACATATCTTAT-3′
RPS12un-intA20	AS	5′-AAAAACATATTTTTTTTTTTTTTTTTTTTCTTATTCTAAAATC-3′
All A6un	S	5′-**TGTAATACGACTCACTATAGGG**GGGGAATTTTGAGGAGATTCTTG-3′
A6un	AS	5′-TATTATTAACTTATTTGATCTTATTC-3′
A6un-A20	AS	5′-TTTTTTTTTTTTTTTTTTTTTTATTATTAACTTATTTGATCTTATTC-3′
All RBP16	S	5′-**TGTAATACGACTCACTATAGGG**TTTAAAGGAGAACGAGAAGATG-3′
RBP16	AS	5′-CTGACAAATAACGGACTTC-3′
RBP16-A20	AS	5′-TTTTTTTTTTTTTTTTTTTTCTGACAAATAACGGACTTC-3′

editing sites (11). In addition, the poly(A) tail lengths on specific mRNAs are regulated in a life cycle stage-specific manner (12, 14–16). This suggests that polyadenylation of mitochondrial mRNAs has an important regulatory function during trypanosome development.

We previously employed *in organello* pulse-chase experiments to study the role of polyadenylation and mRNA stability in regulating *T. brucei* mitochondrial gene expression (10). These assays revealed two distinct mRNA turnover pathways in *T. brucei* mitochondria. The first pathway involves specific and rapid degradation of polyadenylated mRNAs and requires the addition of UTP. The second pathway mediates slow degradation of mRNAs and is not dependent on the presence of a poly(A) tail or the addition of exogenous UTP. These studies suggested that mRNA 3′-poly(A) tails can act as *cis*-acting elements to facilitate RNA decay in *T. brucei* mitochondria. To test this hypothesis, we developed an *in vitro* assay that allows us to directly examine the roles of specific 3′-sequences in RNA decay. We found that a salt-extracted mitochondrial membrane fraction preferentially degraded polyadenylated mitochondrially and non-mitochondrially encoded RNAs over their non-adenylated counterparts. Turnover of unedited mitochondrial RNAs was stimulated by poly(A) tails as short as 5 nucleotides, although an *in vivo* tail length of 20 adenosines supported the most rapid decay. In addition, the nuclease activity was slowed by insertion of uridines into the poly(A) tail and delayed by internalization of the poly(A) tract. Finally, we show that poly(A)-specific degradation proceeded in the 3′ to 5′ direction by the action of a hydrolytic exonuclease. These results define the 3′-poly(A) tail as a *cis*-acting element that promotes RNA degradation in *T. brucei* mitochondria, thereby providing support for the model that polyadenylation can destabilize trypanosome mitochondrial mRNAs *in vivo*. Furthermore, our studies suggest that polyadenylation may be a general mechanism by which degradation of mitochondrial RNAs is mediated.

EXPERIMENTAL PROCEDURES

Cell Culture and Mitochondrial Isolation—Procyclic form *T. brucei brucei* clone IsTaR1 stock EATRO 164 was grown as described (23). Mitochondrial vesicles were isolated on 20–35% linear Percoll gradients and stored at −80 °C (24).

Mitochondrial Extract Preparation—Percoll gradient-purified mitochondrial vesicles were thawed on ice and collected by centrifugation at 13,000 rpm for 10 min at 4 °C in a Heraeus Instruments Biofuge Pico. Pelleted mitochondrial vesicles were resuspended in Buffer A (20 mM Tris-HCl (pH 7.5), 50 mM KCl, 1 mM EDTA, 10% glycerol, and 1 mM dithiothreitol) at a concentration of 2×10^{10} cell eq/ml. All buffers contained a protease inhibitor mixture (1 mM phenylmethylsulfonyl fluoride, 1 μg/ml leupeptin, and 5 mM iodoacetamide). Vesicles were lysed at 4 °C for 10 min in Buffer A containing 0.2% Nonidet P-40. The resulting mitochondrial lysate was used for *in vitro* degradation assays or centrifuged at 100,000 × *g* for 1 h at 4 °C. The supernatant (S100) was recovered and stored at −80 °C for use in enzymatic assays. The pellet (membrane fraction) was resuspended in 2 ml of Buffer A containing 0.2% Nonidet P-40 and then centrifuged at 100,000 × *g* for 30 min at 4 °C. The pellet (washed membrane fraction) was resuspended at a concentration of 2×10^{10} cell eq/ml in Buffer A containing 0.2% Nonidet P-40 and 1 M KCl to extract peripheral membrane proteins. This resuspension was homogenized with a B-type pestle and Dounce and then incubated for 1 h at 4 °C with constant rotation. The homogenized extract was centrifuged at 100,000 × *g* for 1 h at 4 °C. The supernatant (salt-extracted membrane protein (EMP)[1]) was dialyzed against 1 liter of Buffer A and stored at −80 °C for use in enzymatic assays. The poly(A)-specific nuclease activity present in this fraction (see "Results") was stable for ~1 month at −80 °C. The pellet from the last centrifugation step (insoluble membrane protein) was dialyzed into Buffer A and stored at −80 °C for later use. Protein quantification was performed with the Bio-Rad protein assay using bovine serum albumin as a standard.

In Vitro Transcription—All RNAs were synthesized by *in vitro* transcription from PCR-generated templates, created using the primers indicated in Table I, with the exception of pBluescript II SK⁻ RNA. The sense primers all contain a region complementary to the RNA of interest and a T7 promoter region (shown in boldface in Table I). The antisense primers contain a region complementary to the RNA of interest and an extension of appropriate length and composition to produce the RNAs indicated in Table I. The plasmid pBluescript II SK⁻ (referred to as pBSC; Stratagene) was linearized by digestion with *Bam*HI to serve as a template for synthesis of a 77-nucleotide RNA. To generate the template for *in vitro* transcription of pBSC-A20, pBSC was amplified by PCR using the primers indicated in Table I. The plasmid used to generate the 218-nucleotide RBP16 PCR products with or without a 20-adenosine 3′-extension was previously described (25). The plasmid RPS12-U (10) was used as a PCR template to generate a 221-nucleotide RPS12un (where "un" is unedited) RNA without or with 3′-extensions, except for RPS12un-intA20 (where "int" is internal).

The pRPS12unAI9 plasmid (a plasmid containing 20 adenosine residues inserted 9 bp from the 3′ terminus of the complete 221-nucleotide RPS12un RNA) was used as a template for generation of RPS12un-intA20 PCR products. This plasmid (pRPS12unAI9) was created by PCR amplification of RPS12-U with primers RPS12unAI9–5′ (5′-GCGAATTCCTAATACACTTTTGATAACAAACTAAAGTAAA-3′) and

[1] The abbreviations used are: EMP, salt-extracted membrane protein; RPS12, ribosomal protein S12; RBP16, RNA-binding protein of 16 kDa.

RPS12unAI9–3′ (5′-GCGGATCCAAAAACATATTTTTTTTTTTTTTTT-TTTTCTTATTCTAAAATC-3′). Amplified reaction products were digested and ligated into the *Eco*RI/*Bam*HI sites of pBSC to create plasmid pRPS12unAI9.

For generation of A6un (where "A6" is ATPase-6) PCR products, we initially created plasmid pA6un-3′-221. The pA6un-3′-221 plasmid was generated by PCR amplification of *T. brucei* genomic DNA primed with A6un-221–5′ (5′-GCGAATTCGGGGAATTTTGAGGAGATTCTTG-3′) and A6un-221–3′ (5′-GCGGATCCTATTATTAACTTATTTGATCTTAT-TC-3′). This amplification created a product corresponding to the 3′ 221 nucleotides of the unedited ATPase-6 sequence containing exogenous 5′-*Eco*RI and 3′-*Bam*HI restriction sites. This amplified sequence was digested and ligated into the *Eco*RI/*Bam*HI sites of pBSC to create pA6un-3′-221.

RNA was synthesized from the templates described above with T7 RNA polymerase and radioactively labeled with [α-^{32}P]UTP using the Megascript *in vitro* transcription system (Ambion Inc.). Labeled RNAs were separated on 7 M urea and 6% acrylamide denaturing gels and visualized by autoradiography or UV shadowing. Full-length products were excised, eluted from the gel, and concentrated by isopropyl alcohol precipitation.

In Vitro Degradation Assays—RNA degradation activity was initially characterized in the mitochondrial lysate, S100 fraction, EMP fraction, and insoluble membrane protein fraction (see Fig. 1*A*) (data not shown). Assays were carried out in 25 μl of Buffer A containing 1 mM UTP, and 2.5 pmol of both RPS12un and RPS12un-A20 RNAs. UTP was added to each assay to account for the previously observed *in organello* requirement of the rapid poly(A)-specific turnover pathway for this nucleotide (10). Initial reactions for all fractions were started by the addition of 12.5 μg of protein to RNAs and incubation at 27 °C for the times indicated. Reactions were stopped by the addition of 5 μl of stop buffer (50 mM EDTA and 0.2% SDS) and extracted with phenol/chloroform/isoamyl alcohol (25:24:1) using phase lock gels (Eppendorf). The entire aqueous phase was added to 20 μl of 90% formamide loading buffer and heated for 3 min at 90 °C. Equal volumes of each reaction were then analyzed by electrophoresis on a 7 M urea and 6% acrylamide gel and autoradiography. Non-saturated autoradiographs were analyzed using a Bio-Rad GS-700 imaging densitometer and Multi-Analyst software (Version 1.1). Percent full-length RNA remaining was determined by analyzing the density of areas corresponding to full-length RNAs. All other reactions (see Figs. 1*B*–8) were performed as described above, except that RNAs were assayed in separate tubes.

After the initial detection of poly(A)-specific RNA degradation activity in the EMP fraction, reaction conditions were optimized to favor poly(A)-specific activity by altering the KCl concentration in Buffer A to 100 mM (data not shown). Because activity varied between preparations, each EMP preparation was initially characterized by a protein titration. To characterize EMP degradation activity, different amounts of protein were added to a reaction containing Buffer A with 100 mM KCl, 1 mM UTP, and 2.5 pmol of RPS12un or RPS12un-A20. This protein titration was performed after production of each new EMP preparation to determine the optimal amount of protein for use in subsequent time course reactions. All other conditions and procedures were as described above. All experiments were performed at least three times, and data presented are from a single representative experiment.

5′- and 3′-Labeling of RNA—To generate end-labeled RNA, both RPS12un and RPS12un-A20 were synthesized using the Megascript *in vitro* transcription system in the absence of radiolabeled nucleotides. Full-length unlabeled transcripts were resolved and purified as described above, with the exception that all RNAs were visualized by UV shadowing. These unlabeled transcripts then served as reagents for production of both 5′- and 3′-end-labeled RNAs.

To label both RPS12un and RPS12un-A20 transcripts at their 5′-ends, unlabeled RNAs were first dephosphorylated by calf intestinal alkaline phosphatase (Promega). These dephosphorylated transcripts were then labeled with [γ-^{32}P]ATP by T4 polynucleotide kinase (Invitrogen) under forward reaction conditions. Full-length radiolabeled RPS12un and RPS12un-A20 were visualized by autoradiography and gel-purified as described above.

To label the RPS12un and RPS12un-A20 transcripts at their 3′-ends, unlabeled RNAs were incubated with [5′-^{32}P]pAp (ICN) and T4 RNA ligase (Promega) following the manufacturer's recommendations. Labeled RNAs were gel-purified as described above for the 5′-labeled transcripts. Following this labeling reaction, half of the RNAs were dephosphorylated with calf intestinal alkaline phosphatase to remove the 3′-phosphate and to restore the native 3′-OH. This dephosphorylated RNA was purified by phenol/chloroform extraction and concentrated by ethanol precipitation.

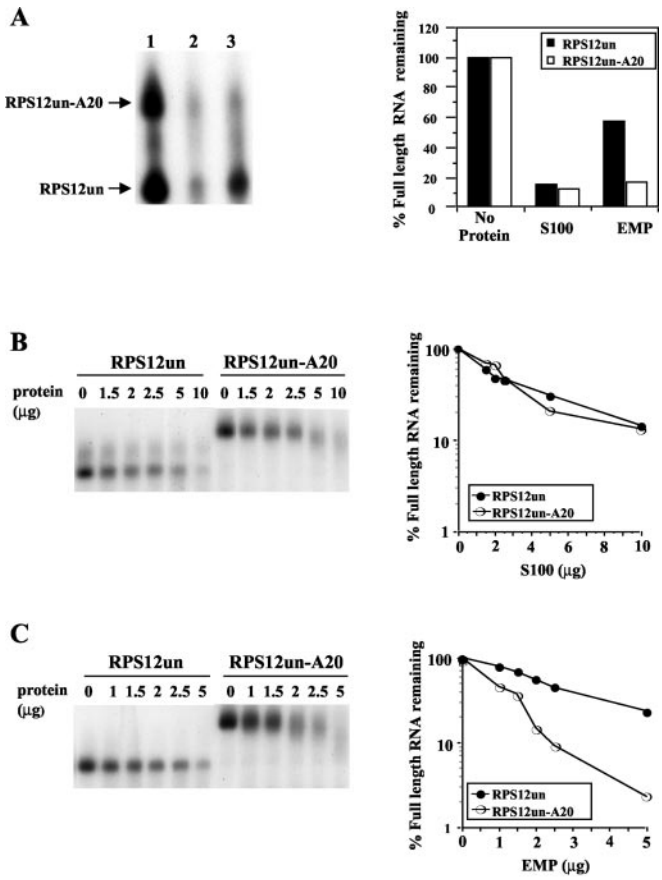

FIG. 1. **Ribonucleolytic activity of mitochondrial protein fractions.** *A*, *in vitro* transcribed and internally labeled RPS12un and RPS12un-A20 (2.5 pmol of each) were incubated in the same reaction for 1 h at 27 °C with buffer (*lane 1*), the mitochondrial S100 fraction (*lane 2*), or the mitochondrial EMP fraction (*lane 3*). Products were separated on a 7 M urea and 6% acrylamide gel and visualized by autoradiography in the *left panel*. The migration positions of the starting materials are indicated to the left. Percent full-length RNA remaining is graphed in the *right panel*. *B*, internally labeled RPS12un and RPS12un-A20 (2.5 pmol of each) were incubated separately with the indicated amounts of mitochondrial S100 fraction for 1 h at 27 °C. Starting materials are shown in the *0 protein lanes*. Products were separated and visualized as described for *A*. The autoradiograph is shown in the *left panel*, and the results from analysis of the data are plotted on the graph in the *right panel*. *C*, RNAs were subjected to the same protocol as described for *B*, except that they were incubated with the EMP fraction.

Thin Layer Chromatography—In vitro RNA degradation reactions were performed as described above and stopped by the addition of formic acid to a final concentration of 1 N. The method of Bochner and Ames (26) was adapted to separate nucleotide products. In brief, a total of 10 μl of formic acid-extracted nucleotides were spotted onto polyethyleneimine-F-cellulose (J. T. Baker Inc.) in 5-μl aliquots, allowing drying between each aliquot. Plates were soaked in methanol and air-dried, and nucleotides were resolved using 0.75 M Tris and 0.45 M HCl. Plates were washed with methanol for 20 min, air-dried, and visualized by autoradiography. To define resolution of nucleotides, 2-μl aliquots of 10 mM marker nucleotides were spotted onto the same plates with samples, resolved as described above, and visualized by UV shadowing.

RESULTS

Localization of a Mitochondrial Ribonuclease Activity That Preferentially Degrades Polyadenylated RNAs—To examine the mechanisms underlying the poly(A)-specific pathway of RNA turnover observed *in organello*, we developed an *in vitro* RNA turnover system. In this assay, *in vitro* transcribed body-labeled RNAs were incubated with mitochondrial lysate or fractions thereof. RNA degradation was monitored by gel electrophoresis, followed by autoradiography. Ribonucleolytic ac-

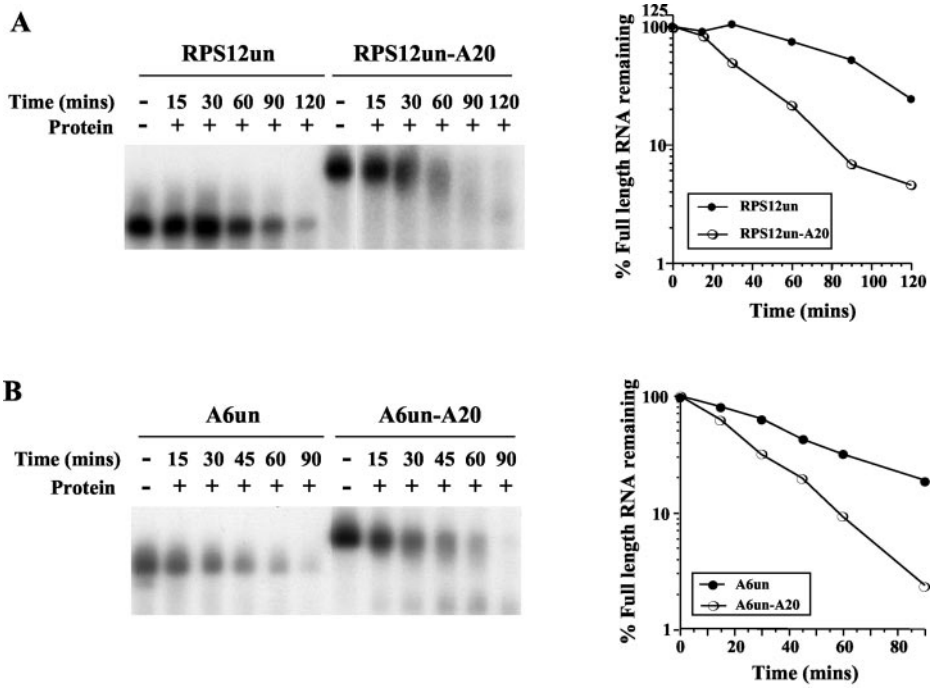

FIG. 2. **Mitochondrially encoded RNAs with 3′-poly(A) extensions degrade more rapidly than their corresponding non-adenylated RNAs.** RPS12un RNA (*A*) and the 3′ 221 nucleotides of A6un RNA (*B*) either with or without a 20-nucleotide poly(A) tail were internally labeled. These RNAs were incubated with the mitochondrial EMP fraction at 27 °C for the indicated times. Products were resolved on a 7 M urea and 6% acrylamide gel and visualized by autoradiography in the *left panels*. The − *Protein* and − *Time (mins) lanes* indicate starting materials. Percent full-length RNA remaining was determined by densitometry and is plotted for each time point in the *right panels*.

tivity was initially characterized by incubation of mitochondrial fractions with *in vitro* transcribed RNA derived from the unedited mitochondrial transcript for ribosomal protein S12 (RPS12) either lacking or containing a 20-adenosine 3′-extension (RPS12un and RPS12un-A20, respectively). The tail length of 20 adenosine residues was chosen to approximate tail lengths observed *in vivo* for *T. brucei* unedited mitochondrial transcripts (11, 12, 14–16, 21). Turnover rates of polyadenylated RPS12un RNAs were compared with those of the same RNAs lacking a poly(A) tail.

We began by examining the ribonucleolytic activity present in total mitochondrial lysate. The lysate was incubated with either RPS12un or RPS12un-A20 for 1 or 3 h. At both time points, total mitochondrial lysate demonstrated robust nonspecific ribonucleolytic activity (data not shown). To separate nonspecific and predicted poly(A)-specific ribonuclease activities, the lysate was fractionated into soluble, salt-extracted membrane, and integral membrane fractions as described under "Experimental Procedures." The three fractions obtained by this procedure were incubated with RPS12un and RPS12un-A20 RNAs in the same reaction for 1 h (Fig. 1*A*) (data not shown). Ribonuclease activity was detected in the soluble protein fraction (S100) and the EMP fraction (Fig. 1*A*). The insoluble membrane protein fraction contained no detectable ribonucleolytic activity (data not shown). Intriguingly, although the S100 fraction displayed a nonspecific RNA degradation activity, the EMP fraction exhibited a 3-fold preferential degradation of RPS12un-A20 (Fig. 1*A*). To confirm the presence of an activity that preferentially degrades polyadenylated RNAs in the EMP fraction, we performed reactions in which non-adenylated and adenylated RPS12un RNAs were incubated separately over a wide range of protein concentrations (Fig. 1*B*). Only nonspecific ribonucleolytic activity was observed with the S100 fraction at all tested protein levels from 1.5 to 10 μg. Conversely, preferential decay of RPS12un-A20 was observed in the EMP fraction at all protein concentrations tested (Fig. 1*C*). Differential decay of adenylated and non-adenylated RNAs increased with increasing amounts of EMP from a 1.7-fold difference at 1 μg to a 10-fold difference at 5 μg (Fig. 1*C*). Thus, *T. brucei* mitochondria contain a membrane-associated activity that preferentially degrades polyadenylated RNAs over their non-adenylated counterparts. The EMP fraction was used in all subsequent experiments.

A 20-Nucleotide Poly(A) Tail Is Sufficient to Mediate Preferential Turnover of Both Mitochondrial and Non-mitochondrial RNAs—We next asked whether facilitation of RNA turnover by a 3′-poly(A) tract is a specific feature of RPS12un RNA or whether it can be extended to other mitochondrial or non-mitochondrial RNAs. We first compared the degradation rates of RPS12un and RPS12un-A20 with those of another mitochondrial RNA. To this end, the 221 nucleotides of the 3′-end of unedited ATPase-6 mitochondrial RNA were synthesized without or with a 20-nucleotide 3′-poly(A) extension (A6un and A6un-A20, respectively). Time course experiments performed with RPS12un and RPS12un-A20 revealed a preferential decay of RPS12un-A20 (Fig. 2*A*). In the experiment presented in Fig. 2*A*, RPS12un-A20 degraded with a half-life of 30 min, whereas RPS12un degraded more slowly with a half-life of 92 min. Over several experiments, we observed a 2.0 ± 0.3-fold (n = 16) difference in half-life between RPS12un and RPS21un-A20. The maximum observed difference in percent full-length RNA remaining was 7.5-fold at 120 min (Fig. 2*A*). Similarly, the ribonuclease activity of the EMP fraction degraded A6un-A20 more rapidly than unmodified A6un (Fig. 2*B*). In the experiment shown in Fig. 2*B*, the half-lives were 39 min for A6un and 21 min for A6un-A20. Data from several experiments showed that A6un had a 1.9 ± 0.1-fold (n = 3) longer half-life than A6un-A20. The greatest difference in percent full-length RNA remaining between A6un and A6un-A20 was 7.8-fold at 90 min (Fig. 2*B*).

To determine whether the poly(A) tail is sufficient to facilitate rapid RNA turnover or whether mitochondrially encoded *cis*-acting sequences are required, we examined degradation of two transcripts not encoded in the mitochondrial genome of *T. brucei* (Fig. 3). A 77-nucleotide portion of the pBSC vector was used to create RNA with or without a poly(A) tail (pBSC-A20 and pBSC, respectively). The pBSC RNAs were incubated with EMP, and reactions were stopped at different times. Similar to what was observed with native transcripts, pBSC RNAs containing a poly(A) tail were more rapidly degraded than their non-tailed counterparts by the activity contained in the EMP fraction (Fig. 3*A*). Polyadenylated pBSC RNA degraded with a

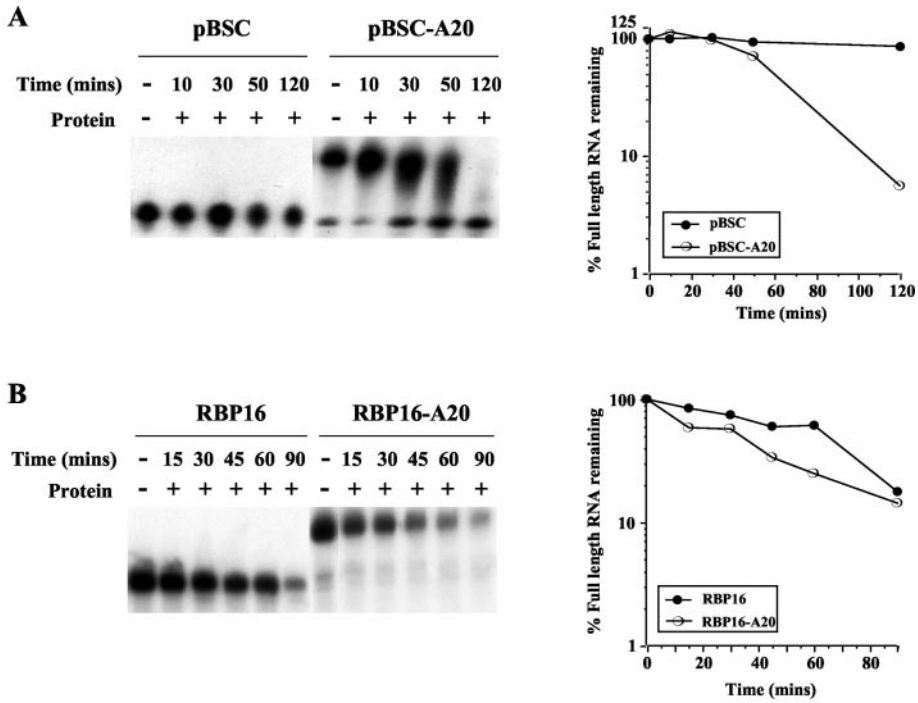

FIG. 3. **The poly(A) tail is sufficient to stimulate preferential degradation of non-mitochondrially encoded RNAs.** Internally labeled RNAs were incubated with the mitochondrial EMP fraction at 27 °C for the indicated times. Products were resolved on a 7 M urea and 6% acrylamide gel and visualized by autoradiography in the *left panels*. The − *Protein* and − *Time (mins) lanes* indicate starting materials. Percent full-length RNA remaining was determined by densitometry and is plotted in the *right panels*. *A*, RNAs were created from a 77-nucleotide portion of the pBSC vector. RNAs were synthesized with (pBSC-A20) or without (pBSC) a 20-adenosine 3′-extension. *B*, RNAs were synthesized from a 218-bp region of *T. brucei* RBP16 nuclear transcript either without (RBP16) or with (RBP16-A20) a 20-nucleotide poly(A) tail.

half-life of 72 min in the experiment presented. However, non-tailed pBSC RNA did not degrade below 80% remaining in our assays, making determination of differences in half-life impossible (Fig. 3*A*). Degradation of pBSC-A20 led to an accumulation of RNAs the size of non-adenylated pBSC RNA, suggesting that decay pauses after removal of the 20-adenosine tail (Fig. 3*A*). Analysis of pBSC RNA sequence by m-fold (27) revealed stable secondary structures throughout the RNA that may account for the accumulation of deadenylated RNA during degradation of pBSC-A20 and the inability of EMP to degrade pBSC RNA. Therefore, using m-fold analysis (27), we selected an unstructured 218-bp region of the *T. brucei* nuclear transcript RBP16 (25) to serve as a template for synthesis of RNA without or with a 20-nucleotide poly(A) tail (RBP16 and RBP16-A20, respectively). As observed with the previous transcripts, the ribonucleolytic activity of EMP more rapidly degraded RBP16-A20 RNA than RBP16 RNA, with half-lives of 35 and 67 min, respectively (Fig. 3*B*). The average difference in half-live between these two RNAs was 2.0 ± 0.2-fold ($n = 3$), similar to the difference in half-life observed for adenylated and non-adenylated mitochondrial RNAs. However, the greatest difference in percent full-length RNA remaining between RBP16 and RBP16-A20 was only 2.5-fold at 60 min (Fig. 3*B*). These results demonstrate that a 20-adenosine tail is sufficient to stimulate rapid degradation of mitochondrial or non-mitochondrial transcripts *in vitro*.

Role of Poly(A) Tail Length in Mediating RNA Turnover—In our next set of experiments, we determined the minimum poly(A) tail length capable of supporting preferential RNA degradation. Using different antisense primers (Table I), templates were constructed to synthesize RPS12un transcripts without a 3′-extension or with a 5-, 10-, 15-, or 20-nucleotide poly(A) extension. These five transcripts were then incubated separately with the EMP fraction, and their decay was measured over a time course. As expected, RPS12un remained relatively stable, whereas RPS12un-A20 degraded rapidly (Fig. 4). In addition, we consistently observed that poly(A) tails of 5, 10, or 15 nucleotides supported more rapid degradation of their transcripts compared with the non-tailed RNA (Fig. 4). The difference in degradation rates observed between RNAs possessing 5-, 10-, or 15-nucleotide extensions did not always strictly correlate with their tail length (Fig. 4) (data not shown). However, poly(A) tails of 5–15 nucleotides were never as effective in stimulating degradation compared with a 20-nucleotide poly(A) tail (Fig. 4) (data not shown). These results indicate that the factors that stimulate poly(A)-specific degradation must have the ability to bind or recognize a sequence as short as 5 nucleotides. However, the native tail length of 20 nucleotides provides optimal stimulation of RNA decay.

Having demonstrated that shortened poly(A) tails suboptimally stimulated RNA degradation activity *in vitro*, we next investigated whether lengthening the poly(A) tail beyond 20 nucleotides leads to an additional stimulation of the rate of *in vitro* RNA degradation. Poly(A) tail lengths of 30 nucleotides have been observed on partially edited RPS12 transcripts by 3′-rapid amplification of cDNA ends.[2] Thus, RPS12un RNA was synthesized without a 3′-extension or containing a 20- or 30-adenosine extension. These transcripts were then added to the *in vitro* degradation assay, and RNA turnover was measured over time. Both adenylated transcripts were degraded more rapidly than non-adenylated RPS12un (Fig. 5). In general, the degradation rate of RPS12un RNA possessing a 30-nucleotide tail did not significantly differ from that of RPS12un-A20. This indicates that a tail of 20 adenosines optimally stimulates RNA turnover and that the degradation rate is not facilitated by incrementally increasing poly(A) tail length beyond 20 nucleotides.

Role of 3′-Tail Sequence in Stimulating RNA Turnover—mRNA poly(A) tails in *T. brucei* mitochondria often contain interspersed uridine residues (12, 14, 28–30). Moreover, there has been one report of unedited RNAs with 3′-tails composed solely of uridine residues (28). We generated two additional RNAs to examine the effect of 3′-uridine residues on RNA decay rates in EMP. RPS12un RNAs were synthesized without a 3′-extension or with a 20-uridine extension, a 20-adenosine extension, or a mixed extension of adenosines and uridines (Fig. 6*A*). The sequence for RPS12un-AU is the same

[2] L. K. Read, unpublished data.

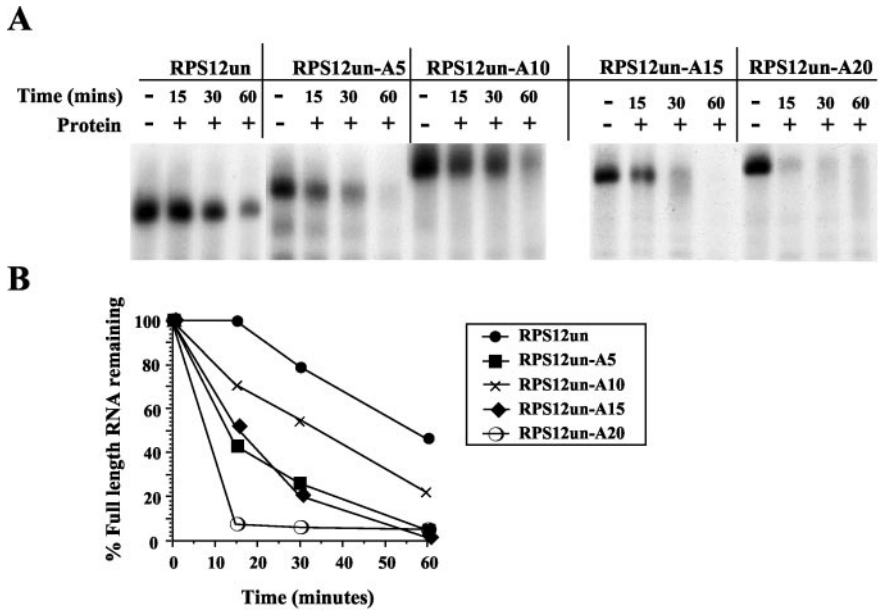

FIG. 4. **Tails as short as 5 adenosines can stimulate RNA degradation.** *A*, internally labeled RPS12un RNAs without a 3′-extension or with a 5-, 10-, 15-, or 20-adenosine extension (RPS12un-A5, RPS12un-A10, RPS12un-A15, and RPS12un-A20, respectively) were incubated with the mitochondrial EMP fraction at 27 °C for the indicated times. Products were resolved on a 7 M urea and 6% acrylamide gel and visualized by autoradiography. The − *Protein* and − *Time (mins) lanes* indicate starting materials. *B*, the data from *A* were analyzed by densitometry, and percent full-length RNA remaining is plotted.

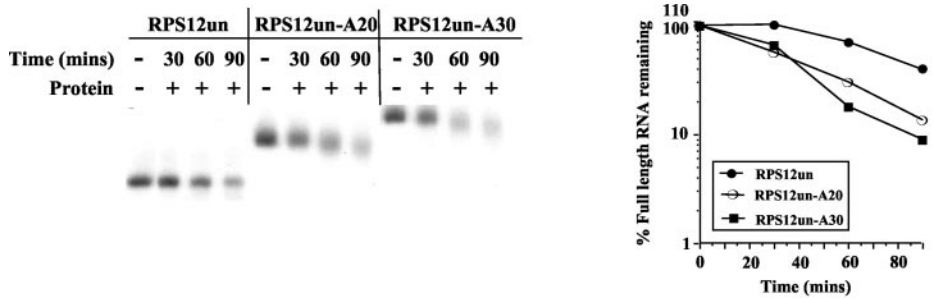

FIG. 5. **Lengthening the poly(A) tail beyond 20 nucleotides does not stimulate more rapid degradation.** Internally labeled RPS12un RNAs without a 3′-extension (RPS12un) or containing a 20- or 30-adenosine extension (RSP12un-A20 and RSP12un-A30, respectively) were incubated with the mitochondrial EMP fraction at 27 °C for 30, 60, or 90 min. Products were resolved on a 7 M urea and 6% acrylamide gel and visualized by autoradiography in the *left panel*. The − *Protein* and − *Time (mins) lanes* indicate starting materials. Percent full-length RNA remaining was determined by densitometry and is plotted in the *right panel*.

as that of a partially edited RPS12 cDNA clone previously obtained by 3′-rapid amplification of cDNA ends.[2] These four transcripts were added separately to *in vitro* degradation assays, and RNA turnover was measured at 30-min intervals. RPS12un RNA with a 20-uridine tail was generally degraded at a rate similar to that of non-adenylated RPS12un (Fig. 6, *B* and *C*). Both of these RNAs were degraded more slowly than RPS12un-A20. RPS12un containing a mixed AU tail degraded at an intermediate rate between those of adenylated and non-adenylated RPS12un RNAs (Fig. 6, *B* and *C*). The intermediate degradation supported by the AU tail is reminiscent of results obtained for the 5-, 10-, and 15-nucleotide poly(A) extensions (Fig. 4). Thus, the addition of uridines to the poly(A) tail may reset recognition by the degradation machinery to the 9 adenosines 3′ of the uridine stretch (Fig. 6*A*). Whether a uridine stretch of less than 4 nucleotides, as is often observed *in vivo*, would have a similar effect is unknown. Nevertheless, these results imply that uridines inserted into a poly(A) tail may act to restructure the poly(A) tail in a manner that slows the degradation machinery.

Decay Is Delayed if the Poly(A) Element Is Not Located at the 3′-End of the RNA—We next examined whether a poly(A) tail must be located at the 3′-end of an RNA to stimulate its rapid degradation. To test this, RPS12un was modified to generate RPS12un with a 20-adenosine stretch 9 nucleotides from the 3′-end of the RNA (RPS12un-intA20). This RNA was incubated with the EMP fraction, and decay was measured and compared with that of RPS12un and RPS12un-A20. As observed in previous experiments, RPS12un with a poly(A) tract located at the 3′-end was more rapidly degraded than RPS12un without a poly(A) tract (Fig. 7). RPS12un with an internal poly(A) tract first degraded slowly, at a rate similar to that of RPS12un (Fig. 7). This slow decay was followed by a shift in decay to a rapid turnover rate, similar to that of the rapid degradation observed with RPS12un-A20 (Fig. 7). Transition to a faster decay rate at late time points was consistently observed in reactions with RPS12un-intA20 RNA. These results suggest that decay first occurs in a slow nonspecific manner until the 9 encoded RPS12 nucleotides at the 3′-end of the RNA are removed. Removal of these nucleotides subsequently allows the rapid poly(A)-specific activity to degrade the remainder of the RNA molecule. From these experiments, we conclude that the poly(A) tail must be located at the 3′-end of the RNA to stimulate preferential decay of RPS12un RNA and that internalization of the poly(A) tract causes a delay in degradation.

Directionality of Ribonucleolytic Activity in EMP—To determine the direction of degradation of adenylated RNA, 3′- or 5′-labeled RPS12un-A20 RNAs were incubated separately with EMP, and degradation was monitored over a time course. 5′-Labeled RPS12un-A20 degraded into several intermediate products (Fig. 8*A*). This pattern of decay suggests that degradation occurs by an exonuclease proceeding in the 3′ to 5′ direction and/or by an endonuclease. Degradation of 3′-labeled RPS12un-A20 with a hydroxyl terminus resulted in only a

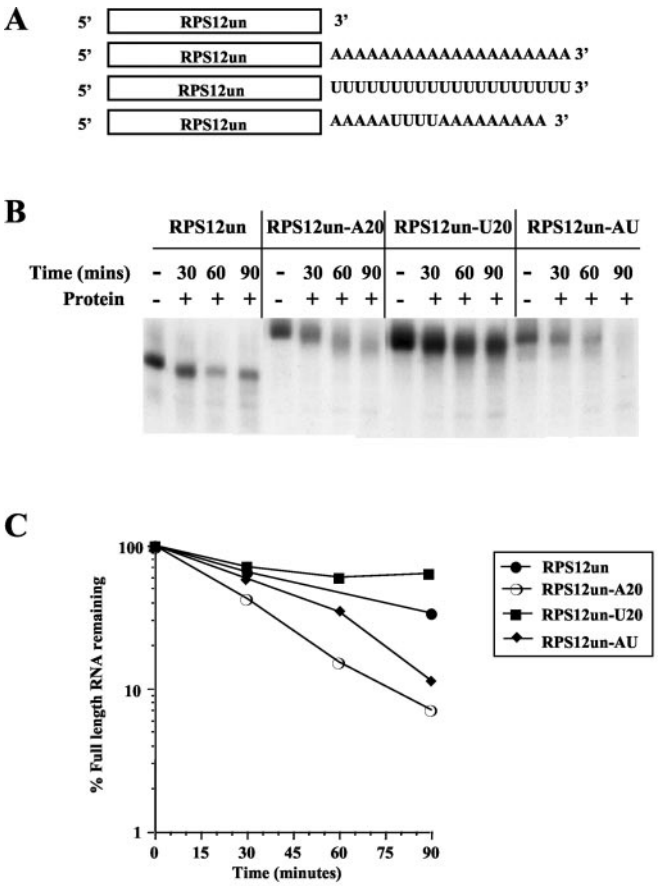

FIG. 6. **A poly(U) tail does not support rapid degradation, and addition of uridines to the poly(A) tail reduces efficiency of poly(A)-stimulated degradation.** *A*, shown is a schematic of the four RNAs used in this experiment. Beginning at the top is a depiction of unmodified RPS12un, RPS12un with a 20-adenosine extension (RPS12un-A20), RPS12un with a 20-uridine extension (RPS12un-U20), and RPS12un with a hybrid adenosine and uridine extension (RPS12un-AU). *B*, each of the four RNAs depicted in *A* was incubated with the mitochondrial EMP fraction at 27 °C for 30, 60, or 90 min. Products were resolved on a 7 M urea and 6% acrylamide gel and visualized by autoradiography. The − *Protein* and − *Time (mins) lanes* indicate starting materials. *C*, the data from *B* were analyzed by densitometry and are plotted as percent full-length RNA remaining.

single product after 60 min of incubation (Fig. 8*B*). No intermediate products were observed even after prolonged exposure of the gel (data not shown). Thin layer chromatographic analysis indicated that the single product released by degradation of 3′-labeled RPS12un-A20 was AMP (Fig. 8*D*). In addition, analysis of products released by degradation of internally labeled RPS12un-A20 by thin layer chromatography revealed comigration of released nucleotides with 5′-UMP (data not shown). Release of mononucleotides with no intermediates confirms that degradation of polyadenylated RPS12un is caused by a 3′–5′-exonuclease. Similar results were observed when reactions were performed with 3′- and 5′-labeled RPS12un RNAs (data not shown).

To further characterize the nuclease activity involved in preferential degradation of polyadenylated RNAs, we next asked whether this activity is inhibited by a 3′-phosphate group. Degradation assays with 3′-labeled phosphorylated RPS12un-A20 demonstrated that the EMP fraction could degrade RNA with a 3′-phosphate terminus to some extent (Fig. 8*C*). However, we also observed an accumulation of intermediate products in addition to the mononucleotide product observed during degradation of 3′-labeled RPS12un-A20 with a hydroxyl terminus (Fig. 8, *B* and *C*). Taken together, these results indicate that the majority of ribonucleolytic activity in the EMP fraction results from a hydrolytic 3′–5′-exonuclease that can degrade adenylated and non-adenylated RNAs. Additionally, an endonuclease and/or a 5′–3′-exonuclease is also present, but this activity is observed only when the major 3′–5′-activity is inhibited by blockage of the 3′-end of the RNA.

DISCUSSION

In this study, we utilized *in vitro* assays to demonstrate that 3′-poly(A) tails are a major determinant of RNA turnover in *T. brucei* mitochondria, in agreement with our previous *in organello* results (10). We identified a poly(A)-specific ribonucleolytic activity that is localized to the mitochondrial membranes of *T. brucei*. By monitoring the turnover of polyadenylated and non-adenylated RNAs *in vitro*, the mechanism by which polyadenylated RNAs are preferentially degraded in this system was characterized. We found that RNAs possessing a 3′-poly(A) extension of as little as 5 nucleotides were degraded more rapidly than their non-adenylated counterparts and that uridine residues inhibited this rapid decay. We have also shown that degradation of polyadenylated RNAs proceeded in the 3′ to 5′ direction through the action of a hydrolytic exoribonuclease.

Plant mitochondrial RNAs can be polyadenylated at their mature 3′-ends, and this modification has been shown to accelerate RNA decay both *in vivo* and *in vitro* (8, 9). A ribonuclease activity that preferentially degrades polyadenylated RNAs has recently been characterized in potato mitochondria (7). In our investigation of *T. brucei* mitochondria, we identified several aspects of preferential poly(A)$^+$ RNA turnover that are similar to the characteristics of the plant mitochondrial activity. First, decay of RNAs by the partially purified plant mitochondrial extract is most efficient when RNAs contain poly(A) tails approximating native lengths (7). Similarly, RNAs with poly(A) tails approximating *in vivo* length (~20 nucleotides) were degraded more efficiently than RNAs containing shorter tails by the *T. brucei* activity. Second, decay of polyadenylated RNA in both plant and *T. brucei* mitochondria involves a 3′–5′-exoribonuclease (7). Third, degradation of polyadenylated RNAs in plant mitochondria proceeds without the formation of a stable intermediate corresponding to RNA with the poly(A) tail removed (7). We also did not observe accumulation of deadenylated RNAs in our system provided that the RNA did not contain significant secondary structure. This is in contrast to what has been observed in mammalian cytoplasmic *in vitro* RNA turnover systems (1). In mammals, it has been established that degradation of cytoplasmic RNA involves separate enzymes for destruction of the poly(A) tail and the body of the RNA (1). The absence of a deadenylated intermediate in the mitochondrial systems suggests a model whereby the poly(A) tract recruits a nuclease complex capable of degrading the entire RNA molecule and not necessarily a poly(A)-specific nuclease that pauses or dissociates from the RNA following deadenylation.

In addition to the similarities between the plant and trypanosome mitochondrial activities, several differences are also apparent. For example, RNAs containing a poly(A) tail of 5 nucleotides were more rapidly degraded than their non-adenylated counterparts. In contrast, 5 adenosine residues are not sufficient to support degradation of RNA by plant mitochondria lysates (7). These systems also differ in the effect of RNA secondary structure on degradation. In our studies, degradation of pBSC RNA with a 20-nucleotide poly(A) tail resulted in the accumulation of a product corresponding in size to pBSC lacking a tail. m-fold analysis (27) of the pBSC transcript revealed the presence of a stable secondary structure in this RNA, strongly suggesting that degradation of polyadenylated RNAs in *T. brucei* mitochondria is inhibited by secondary struc-

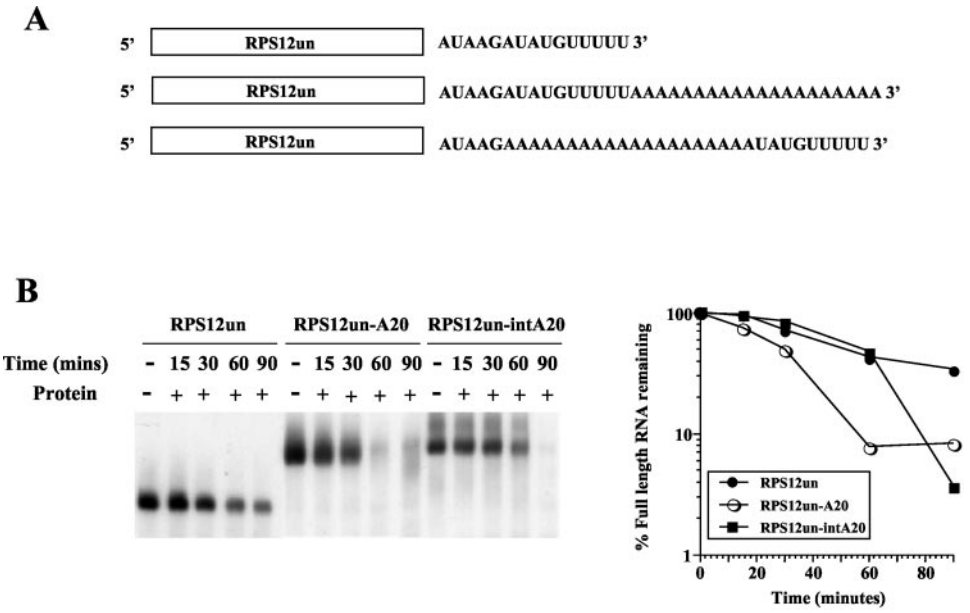

FIG. 7. **Repositioning of the poly(A) tail delays degradation.** *A*, Schematic of the three RNAs used in this experiment. Three RNAs depicted, from top to bottom, are RPS12un without modification, RPS12un with 3′-tail of 20 adenosines (RPS12un-A20) and RPS12un with an internal 20-adenosine tract located 9 nucleotides from the 3′-end (RPS12un-intA20). *B*, Internally labeled RNAs of the species depicted in A were incubated with mitochondrial EMP fraction at 27 °C for the indicated times. Products were resolved on a 7 M urea and 6% acrylamide gel and visualized by autoradiography in the *left panel*. The − *Protein* and − *Time (mins) lanes* indicate starting materials. The data in the *left panel* were analyzed, and percent full-length RNA remaining is plotted at each time point in the *right panel*.

tures. Conversely, the plant mitochondrial activity degrades polyadenylated RNAs without formation of a deadenylated intermediate regardless of the presence of stable secondary structures (7). Another difference between degradation of polyadenylated RNAs in plant and *T. brucei* mitochondria arises from the type of products released in each system. Our investigations show that, upon degradation of RPS12un-A20, ribonucleotide monophosphates are released, demonstrating that RNA degradation in *T. brucei* EMP occurs through a hydrolytic exonuclease. However, degradation of polyadenylated RNA in plant mitochondria releases products characteristic of both hydrolytic and phosphorolytic enzymes (7). This suggests that the activity characterized in this study has been purified to a greater extent than the potato mitochondrial activity, resulting in loss of the phosphorolytic nuclease, or that our purification procedure inactivates the phosphorolytic enzyme. Partially purified plant and *T. brucei* mitochondrial fractions also vary in their ability to degrade RNAs in which the poly(A) tract has been internalized. Placement of the poly(A) tract 9 nucleotides from the 3′-end of the RNA delayed, but did not abolish, RNA degradation in *T. brucei* mitochondria. Conversely, a similar RNA tested in the plant mitochondrial *in vitro* system is completely stable. This difference may result from contaminating nonspecific ribonucleases present in the *T. brucei* EMP preparation that slowly degrade the 3′-end until the poly(A) tail is exposed. The poly(A)-specific activity could then associate with the newly exposed 3′-poly(A) tail. Alternatively, a poorly active ribonuclease may load at the 3′-end of the RNA and encounter a processivity factor associated with the poly(A) tract, thereby triggering the interacting nuclease to rapidly degrade the remainder of the RNA.

The enzymes responsible for degradation of polyadenylated RNAs in plant and *T. brucei* mitochondria are not yet defined. In bacteria and chloroplasts, some of the enzymes involved in poly(A)-specific RNA turnover have been identified. The *Escherichia coli* degradosome component RNase E degrades poly(A) tails and has been shown to interact with poly(A)-binding proteins (2, 31). However, RNase E is an endoribonuclease, and our observations show that decay of polyadenylated RNAs in *T. brucei* mitochondria occurs through an exoribonuclease. Two bacterial exoribonucleases, polynucleotide phosphorylase and RNase II, are known to degrade polyadenylated RNAs in the 3′ to 5′ direction (2, 5). In addition, polynucleotide phosphorylase isolated from chloroplasts preferentially degrades polyadenylated RNAs (3). In our *in vitro* degradation system, nucleotide monophosphates are released by degradation of polyadenylated RNAs, indicating the sole action of a hydrolytic nuclease. Even upon the addition of inorganic phosphate to activate phosphorolytic enzymes, release of nucleotide diphosphates was not observed (data not shown). These results indicate that degradation of polyadenylated RNAs in this system occurs through a hydrolytic enzyme such as RNase II rather than a phosphorolytic enzyme such as polynucleotide phosphorylase. As discussed above, this result stands in stark contrast to poly(A)-specific degradation in plant mitochondria, where RNA degradation has both phosphorolytic and hydrolytic character (7). However, our results do not preclude the possibility that a polynucleotide phosphorylase-like enzyme participates in trypanosome mitochondrial RNA turnover *in vivo*. Indeed, a protein of the expected size that cross-reacts with antibodies against spinach chloroplast polynucleotide phosphorylase (32) is enriched in the EMP fraction of *T. brucei* mitochondria.[3] This enzyme may be inactivated under our current conditions or may require an accessory factor that has been lost during the preparation. The case for the involvement of an RNase II-like activity in our system is strengthened by the profile of products released upon degradation of RNAs containing a 3′-phosphate. With this substrate, although the exonuclease activity is slowed, mononucleotides are released, indicating that our activity has the ability to proceed through the 3′-phosphate. *In vitro* RNA degradation reactions performed with *E. coli* RNase II and RNase R show that these enzymes are also able to degrade RNAs possessing a 3′-phosphate group (33). Taken together, these results suggest that an RNase II- or RNase R-like enzyme in *T. brucei* mitochondria degrades polyadeny-

[3] C.-Y. Kao and L. K. Read, unpublished data.

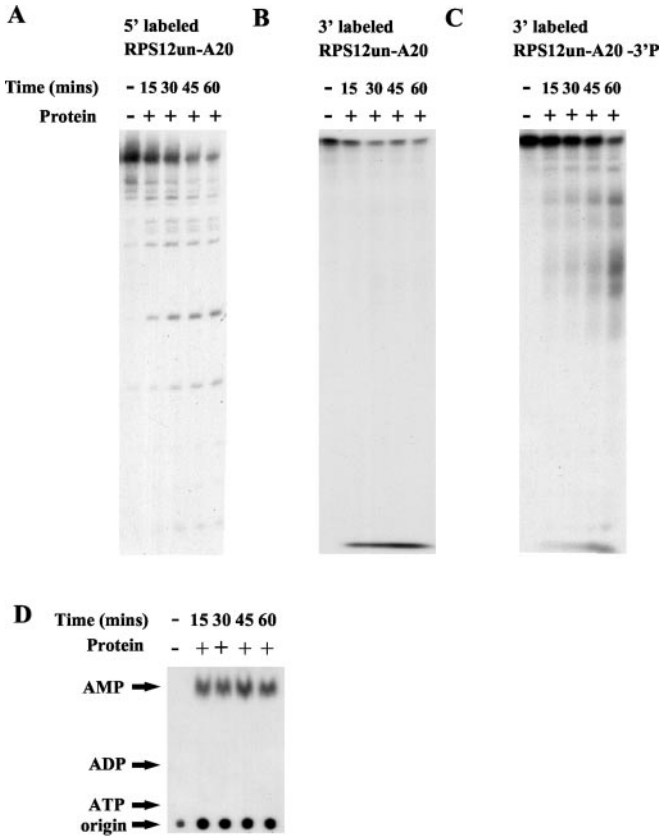

FIG. 8. **Poly(A)-specific degradation proceeds in the 3′ to 5′ direction.** RPS12un-A20 RNAs were labeled at the 3′- or 5′-end and incubated with the mitochondrial EMP fraction at 27 °C for 15, 30, 45, or 60 min. Control lanes containing starting materials are indicated (−). *A*, 5′-labeled RPS12un-A20 was incubated with EMP as described above. Products were resolved on a 7 M urea and 6% acrylamide gel and visualized by autoradiography. *B*, 3′-labeled and dephosphorylated RPS12un-A20 was used in an *in vitro* degradation assay as described above. Products of this reaction were resolved on a 6 M urea and 15% acrylamide gel and visualized by autoradiography. *C*, 3′-labeled RPS12un-A20 possessing a 3′-phosphate group was incubated in an *in vitro* degradation reaction as described for *B*. *D*, products from the assay shown in *B* were spotted onto a polyethyleneimine-F-cellulose plate, resolved using 0.75 M Tris and 0.45 M HCl, and visualized by autoradiography. The migration positions of unlabeled AMP, ADP, and ATP standards are indicated on the left.

lated RNAs. The exoribonuclease component of the yeast mtEXO complex (Dss1p) is homologous to bacterial RNase II and RNase R and functions in mRNA stability and processing *in vivo* (34, 35). A sequence with significant homology to Dss1p is present in the *T. brucei* genome, and we are currently investigating the role of this protein in processing and turnover of *T. brucei* mitochondrial RNAs.

The role of polyadenylation in signaling rapid RNA decay in bacteria and chloroplasts has been well characterized (2, 5, 6). In addition, recent investigations have shown that poly(A) tails stimulate decay of RNAs in plant mitochondria (7, 8). The rapid and specific degradation of polyadenylated RNA fits well with the observation that levels of steady-state polyadenylated transcripts in bacteria (2), chloroplasts (6), and yeast mitochondria (35) are very low. The proportion of RNAs polyadenylated in plant mitochondria is not well defined. However, it has been proposed that these RNAs are expressed at levels comparable to prokaryotic organisms due to the large number of PCR cycles required to amplify cDNAs encoding poly(A) tails (36). In contrast to bacteria, chloroplasts, and yeast or plant mitochondria, polyadenylated RNAs are readily detectable in the steady-state RNA population in trypanosome mitochondria (2, 3, 5, 6, 11–16, 36). In a study designed to identify the proportion of polyadenylated RNAs, we showed that approximately half of the RPS12 RNAs detectable by Northern blotting with an unedited probe contain a poly(A) tail, whereas the remainder are apparently non-adenylated (11). This is similar to what has been reported for human mitochondria, in which the bulk of individual mRNAs are polyadenylated (37) and in which at least one transcript, RNA 17, exists in both adenylated and non-adenylated forms (38). Poly(A)-containing RNAs are degraded in human mitochondria *in vivo* (39), although whether polyadenylated RNAs decay at a faster rate than their non-adenylated counterparts is not known. Since polyadenylated RNAs exist as a significant proportion of the steady-state RNA population in *T. brucei* mitochondria, the presence of a poly(A) tail is unlikely to be the sole trigger for rapid degradation of RNA in this system. Due to the association of our activity with mitochondrial membranes, it is plausible that poly(A)-specific degradation occurs when RNAs are localized to a specific suborganellar compartment where they interact with destabilizing proteins. Localization to sites of RNA turnover may result when RNAs misfold or interact inappropriately with the RNA editing or translational machinery. For example, if an RNA in the process of being edited is prematurely released from the editosome, it could be recognized by its partially edited character and poly(A) tail and be shuttled to the rapid degradation pathway. In this scenario, poly(A)-specific turnover would serve as an RNA surveillance mechanism. Alternatively, rapid degradation of polyadenylated RNAs may result from activation of certain proteins by a change in the physiological state of the mitochondria. Although we did not demonstrate nucleotide dependence in this report, previous work from this laboratory showed that degradation of polyadenylated RNAs *in organello* is stimulated exclusively by UTP (10). An alteration in the parasite's environment that causes a decrease in UTP consumption (by decreasing editing or some other UTP-consuming activity) may activate a protein that stimulates degradation of polyadenylated RNAs. More in-depth studies of *T. brucei* mitochondrial RNA stability will reveal under what circumstances mRNA poly(A) tails are exposed to promote rapid RNA degradation.

Acknowledgments—We thank Chia-Ying Kao and Drs. Margaret Hollingsworth and Michel Pelletier for critical reading of the manuscript. We are also grateful to Katherine Murray for technical assistance and Melissa Miller for important technical suggestions.

REFERENCES

1. Dreyfus, M., and Régnier, P. (2002) *Cell* **111,** 611–613
2. Carpousis, A. J., Vanzo, N. F., and Raynal, L. C. (1999) *Trends Genet.* **15,** 24–28
3. Schuster, G., Lisitsky, I., and Klaff, P. (1999) *Plant Physiol.* **120,** 937–944
4. Bernstein, P., Peltz, S. W., and Ross, J. (1989) *Mol. Cell. Biol.* **9,** 659–670
5. Steege, D. E. (2000) *RNA* (*N. Y.*) **6,** 1079–1090
6. Hayes R., Kudla, J., and Gruissem, W. (1999) *Trends Biochem. Sci.* **24,** 199–202
7. Gagliardi, D., Perrin, R., Maréchal-Drouard, L., Grienenberger, M., and Leaver, C. J. (2001) *J. Biol. Chem.* **276,** 43541–43547
8. Kuhn, J., Tengler, U., and Binder, S. (2001) *Mol. Cell. Biol.* **21,** 731–742
9. Gagliardi, D., and Leaver, C. J. (1999) *EMBO J.* **18,** 3757–3766
10. Militello, K. T., and Read, L. K. (2000) *Mol. Cell. Biol.* **20,** 2308–2316
11. Militello, K. T., and Read, L. K. (1999) *Nucleic Acids Res.* **27,** 1377–1385
12. Souza, A. E., Myler, P. J., and Stuart, K. (1992) *Mol. Cell. Biol.* **12,** 2100–2107
13. Koslowsky, D. J., Bhat, G. J., Perrollaz, A. L., Feagin, J. E., and Stuart, K. (1990) *Cell* **62,** 901–911
14. Read, L. K., Myler, P. J., and Stuart, K. (1992) *J. Biol. Chem.* **267,** 1123–1128
15. Bhat, G. J., Souza, A. E., Feagin, J. E., and Stuart, K. (1992) *Mol. Biochem. Parasitol.* **52,** 231–240
16. Read, L. K., Stankey, K. A., Fish, W. R., Muthiani, A. M., and Stuart, K. (1994) *Mol. Biochem. Parasitol.* **68,** 197–306
17. Koslowsky, D., J., and Yahampath, G. (1997) *Mol. Biochem. Parasitol.* **90,** 81–94
18. Feagin, J. E., Jasmer, D. P., and Stuart, K. (1985) *Nucleic Acids Res.* **13,** 4577–4596
19. Jasmer, D. P., Feagin, J. E., and Stuart, K. (1985) *Mol. Cell. Biol.* **5,** 3041–3047
20. Michelotti, E. F., and Hajduk, S. L. (1987) *J. Biol. Chem.* **262,** 927–932
21. Corell, R. A., Myler, P. J., and Stuart, K. (1994) *Mol. Biochem. Parasitol.* **64,** 65–74
22. Simpson, L., Sbicego, S., and Aphasizhev, R. (2003) *RNA* (*N. Y.*) **9,** 265–276

23. Brun, R., and Schönenberger, M. (1979) *Acta Trop.* **36,** 289–292
24. Harris, M. E., Moore, D. R., and Hajduk, S. L. (1990) *J. Biol. Chem.* **265,** 11368–11376
25. Hayman, M. L., and Read, L. K. (1999) *J. Biol. Chem.* **274,** 12067–12074
26. Bochner, B. R., and Ames, B. N. (1982) *J. Biol. Chem.* **257,** 9759–9769
27. Mathews, D. H., Sabina, J., Zuker, M., and Turner, D. H. (1999) *J. Mol. Biol.* **288,** 911–940
28. Decker, C. J., and Sollner-Webb, B. (1990) *Cell* **61,** 1001–1011
29. Souza, A. E., Shu, H.-H., Read, L. K., Myler, P. J., and Stuart, K. D. (1993) *Mol. Cell. Biol.* **13,** 6832–6840
30. Read, L. K., Wilson, K. D., Myler, P. J., and Stuart, K. (1994) *Nucleic Acids Res.* **22,** 1489–1495
31. Feng, Y., Huang, H., Liao, J., and Cohen, S. N. (2001) *J. Biol. Chem.* **276,** 31651–31656
32. Hayes, R., Kudla, J., Schuster, G., Gabay, L., Maliga, P., and Gruissem, W. (1996) *EMBO J.* **15,** 1132–1141
33. Cheng, Z., and Deutscher, M. P. (2002) *J. Biol. Chem.* **277,** 21624–21629
34. Dziembowski, A., Malewicz, M., Minczuk, M., Golik, P., Dmochowska, A., and Stepien, P. P. (1998) *Mol. Gen. Genet.* **260,** 108–114
35. Dziembowski, A., Piwowarski, J., Hoser, R., Minczuk, M., Dmochowska, A., Siep, M., van der Spek, H., Grivell, L., and Stepien, P. P. (2003) *J. Biol. Chem.* **278,** 1603–1611
36. Lupold, D. S., Caoile, A. G. F. S., and Stern, D. B. (1999) *Plant Cell* **11,** 1565–1577
37. Gaines, G., Rossi, C., and Attardi, G. (1987) *Mol. Cell. Biol.* **7,** 925–931
38. Gaines, G., and Attardi, G. (1984) *Mol. Cell. Biol.* **4,** 1605–1617
39. Avadhani, N. G. (1979) *Biochemistry* **18,** 2673–2678